

## Visualizing Ultrafast Kinetic Instabilities in Laser-Driven Solids using X-ray Scattering

Paweł Ordyna,<sup>1,2,\*</sup> Carsten Bähz,<sup>1</sup> Erik Brambrink,<sup>3</sup> Michael Bussmann,<sup>1</sup> Alejandro Laso Garcia,<sup>1</sup> Marco Garten,<sup>1,4</sup> Lennart Gaus,<sup>1,2</sup> Jörg Grenzer,<sup>1</sup> Christian Gutt,<sup>5</sup> Hauke Höppner,<sup>1</sup> Lingen Huang,<sup>1</sup> Oliver Humphries,<sup>3</sup> Brian Edward Marré,<sup>1,2</sup> Josefine Metzkes-Ng,<sup>1</sup> Motoaki Nakatsutsumi,<sup>3</sup> Özgül Öztürk,<sup>6</sup> Xiayun Pan,<sup>1,2</sup> Franziska Paschke-Brühl,<sup>1</sup> Alexander Pelka,<sup>1</sup> Irene Prencipe,<sup>1</sup> Lisa Randolph,<sup>5,7</sup> Hans-Peter Schlenvoigt,<sup>1</sup> Michal Šmíd,<sup>1</sup> Radka Stefanikova,<sup>1,2</sup> Erik Thiessenhusen,<sup>1,2</sup> Toma Toncian,<sup>1</sup> Karl Zeil,<sup>1</sup> Ulrich Schramm,<sup>1,2</sup> Thomas E. Cowan,<sup>1,2</sup> and Thomas Kluge<sup>1,†</sup>

<sup>1</sup>*Helmholtz-Zentrum Dresden-Rossendorf, Bautzner Landstraße 400, 01328, Dresden, Germany*

<sup>2</sup>*Technical University Dresden, 01069 Dresden, Germany*

<sup>3</sup>*European XFEL, Holzkoppel 4, 22869 Schenefeld, Germany*

<sup>4</sup>*now with Lawrence Berkeley National Laboratory, 1 Cyclotron Rd, Berkeley, CA 94720, USA*

<sup>5</sup>*Universität Siegen, Walter-Flex Straße 3, 57072 Siegen, Germany*

<sup>6</sup>*Universität Siegen, Adolf-Reichwein-Straße 2, 57068 Siegen, Germany*

<sup>7</sup>*now with European XFEL, Holzkoppel 4, 22869 Schenefeld, Germany*

(Dated: April 26, 2023)

Ultra-intense lasers that ionize and accelerate electrons in solids to near the speed of light can lead to kinetic instabilities that alter the laser absorption and subsequent electron transport, isochoric heating, and ion acceleration. These instabilities can be difficult to characterize, but a novel approach using X-ray scattering at keV energies allows for their visualization with femtosecond temporal resolution on the few nanometer mesoscale. Our experiments on laser-driven flat silicon membranes show the development of structure with a dominant scale of 60 nm in the plane of the laser axis and laser polarization, and 95 nm in the vertical direction with a growth rate faster than 0.1/fs. Combining the XFEL experiments with simulations provides a complete picture of the structural evolution of ultra-fast laser-induced instability development, indicating the excitation of surface plasmons and the growth of a new type of filamentation instability. These findings provide new insight into the ultra-fast instability processes in solids under extreme conditions at the nanometer level with important implications for inertial confinement fusion and laboratory astrophysics.

Visualizing, understanding and controlling laser absorption, isochoric heating, particle acceleration, and other relativistic non-linear physics that occur at the interaction of powerful lasers with solids is important for applications ranging from next-generation ion accelerators for medical use[1] to high-energy density physics including laboratory astrophysics[2] and inertial confinement fusion[3, 4]. Only recently, direct drive proton ignition has gained renewed interest as a viable path towards commercialization of Inertial Fusion Energy[5] after the breakthrough fusion ignition achievements at the National Ignition Facility (NIF)[6, 7].

Of special relevance is the understanding and control of plasma instabilities. For example, compression and ignition of fusion targets in indirect-drive experiments carried out e.g. at NIF nanosecond laser rely on the conversion of the laser energy into a homogeneous radiation field by laser-self-generated grating structures

at the hohlraum inner walls[8]. Here we focus on ultrafast few femtosecond relativistic instabilities that are important e.g. for direct drive proton fast ignition fusion [9, 10] that could potentially allow for a much better efficiency. Small fluctuations in the radiation pressure on the pellet surface or in the particle heater pulse would otherwise drive instabilities there, inhibiting maximum compression or heating.

Theories for instabilities in relativistic high-intensity laser interaction with solids fall into two categories: (i) hydrodynamic instabilities growing at interfaces between two fluid-like plasma or photon ensembles, or (ii) kinetic instabilities that occur e.g. when one plasma streams through the other. Whether the one or the other dominate depends on the detailed laser and solid properties. For example, in solids with a structured surface, or driven by lasers with a shallow rising edge laser absorption to relativistic electron currents reaches up to 100%, emphasizing the kinetic streaming instabilities at the front surface [11, 12] or at the rear of the target[13–15], e.g. two-stream instability, Weibel instability, or filamentation. On the other hand, strong hydrodynamic Rayleigh-Taylor-like instabilities

\* p.ordyna@hzdr.de

† t.kluge@hzdr.de

following two-phonon decay or parametric instabilities at the front of plasmas can be dominant for materials consisting of light ions, or driven by ultra-short high-contrast laser pulses, and can break up the laser to electron coupling and inhibit streaming instabilities[16–19].

The physics of these fast few femtosecond, few nanometer plasma instability dynamics and convergence to the micron-scale, picosecond instabilities in high-intensity laser driven solids is one of the large unsolved issues in high-intensity laser plasma science, but its direct observation has previously not been possible because of the small time and few nanometer length scales involved. Microscopic interpretations were therefore primarily based on simulations and indirect measurements, e.g. via optical microscopy [20], interferometry[21], spectroscopy[22], or radiography[13, 14, 23]. Here we demonstrate experimentally that such instabilities indeed exist in the hot solid density plasmas, quantify the strength, and give limits to the growth rate.

Recent advances in the time-resolved diffraction, based on ultra-fast x-ray pulses from XFELs now enable us to investigate laser produced plasmas with nanometer spatial and femtosecond temporal resolution [24–29].

Most of these previous studies focused on the irradiation and ablation of gratings or other pre-structured targets, paving the way towards studies of self-generated non-linear relativistic structural development during the laser irradiation, such as the fast instability growth. Experimental realization of probing the predicted nanoscopic instability growth over few femtoseconds proved difficult, as the world’s most powerful optical drive lasers need to be combined with the most advanced X-ray sources, and experiments faced fundamental challenges such as the parasitic bremsstrahlung generation and self emission of the warm or hot dense plasma that can shadow the signal.

With the recent completion[30] and commissioning of the Helmholtz International Beamline for Extreme Fields (HIBEF[31]) at the EuropeanXFEL[32, 33], the quest for visualising few-femtosecond, few-nanometer scale non-linear plasma dynamics in ultra-short pulse ultra-high intensity (UHI) laser interaction with solids has begun.

One primary goal of HIBEF as well as this work is to provide the novel experimental benchmarks for high energy density science, including the measurement and characterization of kinetic instabilities in

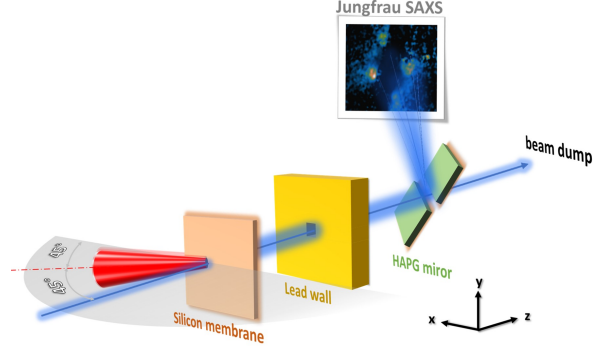


Figure 1. Experimental setup, not to scale. The ReLaX UHI laser (red) is focused onto the Silicon membrane target under  $45^\circ$  in p-polarization, the XFEL (blue) is probing the plasma density under target normal direction. The Jungfrau CCD detector records the SAXS image reflected from the HAPG chromatic mirror.

order to validate codes and to optimize laser absorption and successive processes for above-mentioned applications. HIBEF combines a short-pulse Titanium:Sapphire UHI laser (ReLaX) with the European XFEL beam. The ReLaX laser reaches its highest intensity of  $5 \cdot 10^{20} \text{ W/cm}^2$  when it is focused down to a  $4.7 \mu\text{m}$  (FWHM) focal spot and compressed to  $\tau_L = 30 \text{ fs}$  pulse duration, exceeding the laser intensity at other XFELs by approx. an order of magnitude[34].

We measured time-resolved small angle X-ray scattering (SAXS) patterns with sufficient momentum transfer range that provides with the current setup (Fig. 1) sensitivity for correlation structures up to  $\cong 100 \text{ nm}$ . Since the detector covers only the small angle  $q$ -range, the signal is essentially given by the time integration of the Fourier transform absolute square of the time retarded electron density integrated along the XFEL beam direction

$$I(\mathbf{q}) \propto \int_t |\mathcal{F}_{\mathbf{r}}(E_X(\mathbf{r}, t) \tilde{n}_e(\mathbf{r}, t))|^2 dt, \quad (1)$$

where  $\tilde{n}_e(\mathbf{r}, t) = \int_z n_e(x, y, z, t' = t + z/c) dz$  is the time retarded electron density projection and  $E_X$  is the XFEL amplitude.

Fig. 2 shows the measured scattering patterns as a function of probe delay from probing extremely flat  $2 \mu\text{m}$  thin silicon (Si) membranes irradiated by the ReLaX UHI laser at maximum intensity under  $45^\circ$  angle of incidence and p-polarization. Each main shot was accompanied by a pre-shot and post-shot XFEL-only pulse train on the same spot (for the pre-shots the

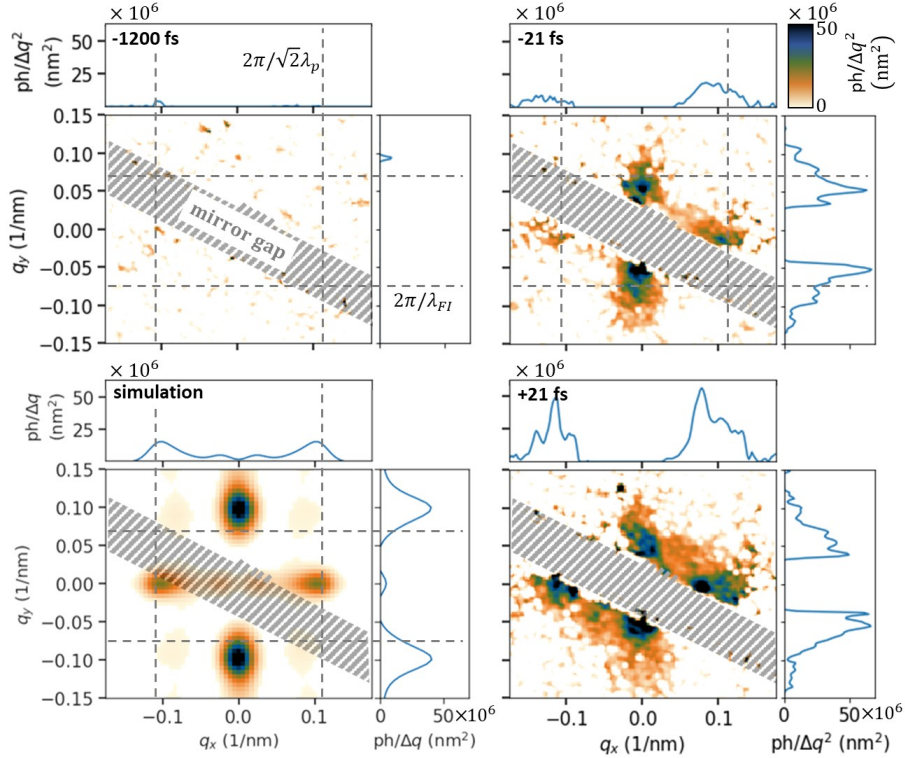


Figure 2. The background subtracted (as determined by an XFEL-only pre-shot train) scattering patterns recorded by the SAXS detector for three exemplary runs (corrected for HAPG mirror reflectivity and geometry, see methods). The respective probe time delay is indicated in the top panels, a simulated scattering pattern is shown for  $t = 0$ . The lineouts were taken through  $q = 0$ , averaged over  $10^{-2}/\text{nm}$ . The dashed lines show the theoretic expectation from filamentation (y-direction) and surface plasmons (x-direction). The relative probe delay given in the top of the panels was extracted from the pulse arrival monitor, with a relative uncertainty below 15 fs (see Methods). The absolute zero delay was defined as the mean value between the two highest signal shots, but was not measured. Profiles are averaged over  $\pm 0.01/\text{nm}$  around  $q = 0$ .

XFEL transmission was reduced by a factor of 0.0006, in order to protect the target from X-ray damage). This enabled us to verify the cold membrane quality, and to subtract parasitic signal in the background. The scattering patterns show dominant signal around the Re-LaX laser peak arrival time along the vertical direction (momentum transfer along the laser magnetic field direction) and horizontal direction (momentum transfer in the plane of the laser axis, the laser electric field vector, and the target normal).

In Fig. 3 we show the integrated number of photons recorded along the horizontal and vertical direction for all the 6 data shots that we took for this study. Note that up to  $-1$  ps no significant scattering was measurable, as expected from a flat membrane. At  $t = -(31 \pm 13)$  fs the signals are still consistent with zero signal within a  $2\sigma$  confidence interval. A large scattering signal then

sharply occurs at  $-(21 \pm 13)$  fs, remaining high for approximately the laser pulse duration. This is an ultra-fast temporal growth of more than two orders of magnitude within  $10 - 30$  fs, which show that the measurements have indeed happened during or shortly after the UHI laser irradiation.

These scattering signals are associated with a growth of periodic plasma electron density modulations on the timescale of only a few femtoseconds. Combining these new observations with simulations shown in Fig. 4, we can attribute the signal in the vertical direction to a two-stream filamentation instability (TSFI) inside the front of the foil, and the horizontal signal to plasmons at the surface and inside the plasma. A synthetic, forward calculated scattering image from our simulations is shown in Fig. 2c.

## DISCUSSION OF THE RESULTS

A cross-like pattern in Fourier space corresponds to a mesh-like pattern in real space. This means that the experimental data directly confirms without any further assumptions that the flat membrane must have developed a corresponding mesh-like electron density pattern in the electron density projected along the XFEL direction according to Eqn. (1) as has long been expected from simulations[35, 36].

This is the first direct measurement of plasma instabilities in high-intensity laser-driven solids during or shortly after the irradiation. One enabling technology that was developed by our group for HIBEF is a SAXS detection system designed primarily to suppress radiation background. Crucially, it consists of a passive radiation background suppression system, i.e. a set of HAPG X-ray crystals[37] between the solid target and the SAXS detector. They act as a chromatic X-ray mirror that separates the signal 8 keV X-ray energy from the background. We thereby effectively suppressed almost any X-ray background and signal from the undriven membrane. Especially at ultra-relativistic laser intensities above  $10^{20}$  W/cm<sup>2</sup> the self emission and bremsstrahlung backgrounds would otherwise have outshone the signal. Additionally, it is quite likely that in earlier studies employing sub-relativistic laser intensity the structure development was not sufficiently strong to be detected. To our knowledge, this is the first study combining a UHI laser, flat solid targets and an XFEL probe, enabling us for the first time to measure the signal generated by relativistic instabilities driven by a UHI short-pulse laser.

To answer the question of the origin of the scattering pattern, we turn to possible instabilities that are known to generate a grating-like pattern. These include, for example, the Rayleigh-Taylor-like (RT), Weibel-like, or filamentation instability, but we could also consider a combination of different waves and instabilities for the different orientations. In fact, since there exists no previous direct measurement of the solid density plasma break up during the ultra-short laser pulse irradiation in literature, we have to resort to simulations of the UHI laser interaction with the silicon membrane in order to identify the plasma dynamics at play.

Our simulation suggests that the scattering signal that corresponds to a mesh-like projected density profile is in fact generated by two rather independent processes that each generate a comb-like density, rotated 90° w.r.t each other, see Fig. 4. First, we find a rapidly growing instability in the *ver-*

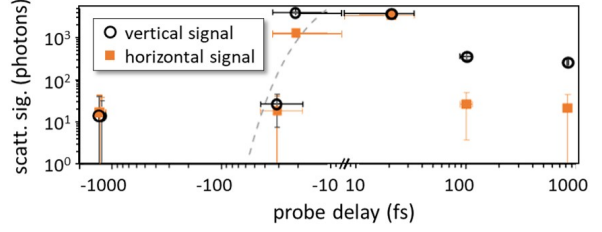


Figure 3. Integrated background subtracted scattering signal strength as a function of probe delay. The projected signal around the peaks was integrated over the scattering signal above the noise level in the respective direction. The probe delay was extracted from the pulse arrival monitor, the relative timing uncertainty is below 15 fs for all shots (absolute timing as in Fig. 2).

*tical direction* (i.e. a density comb in the y-direction with horizontal lines along the x-direction), as witnessed by magnetic field filaments and corresponding density modulations extending inside the target from the front surface. The structure grows within several femtoseconds during the laser irradiation (growth rate  $\Gamma_y^{sim} \cong 0.1$  fs<sup>-1</sup>) and is spatially static, see Fig. 4b. The lower bound for the growth rate extracted from the experiment (dashed line Fig. 3, 1 $\sigma$  confidence interval) is with 0.09/fs in good agreement with the simulation. This structure can be identified as a TSFI of counter-propagating currents (see methods) with an expected filament wavelength of  $\lambda_{FI} = 2\pi\sqrt{\gamma_b}c/\omega_{pe} \cong 90$  nm (dashed horizontal lines in Fig. 2)[38, 39], where  $\gamma_b \approx \pi/2K(a_0^2) = 5.1$  is the Lorentz factor of the laser accelerated electrons[40], and  $\omega_{pe} \cong \sqrt{400}$  is the bulk electron plasma frequency normalized to the laser frequency. The TSFI growth rate is expected to be an order of magnitude larger than observed in the simulation, around 5/fs based on an analytical theory by Bret et al. [11, 35]. Hence we expect that the instability is in continuous saturation and we measure the growth of the saturation limit.

In the *horizontal direction* the simulation shows a dynamic surface electron wave structure moving with the phase velocity  $v_p = c/\sin\Theta$ , where  $\Theta = \pi/4$  is the laser incidence angle w.r.t. the target normal. Along that direction the laser excites surface plasmons, i.e. plasma oscillations in the wake of the laser phase, which then occur as a travelling periodic wave-like density comb with vertical lines at the front with period  $\lambda_p = 2\pi v_p/\omega_{pe} \approx 60$  nm, see right panel in Fig. 4b. It is important to point out that this dynamic feature can only be measured by means of scattering since in shadowgraphic probing the projection of the time-



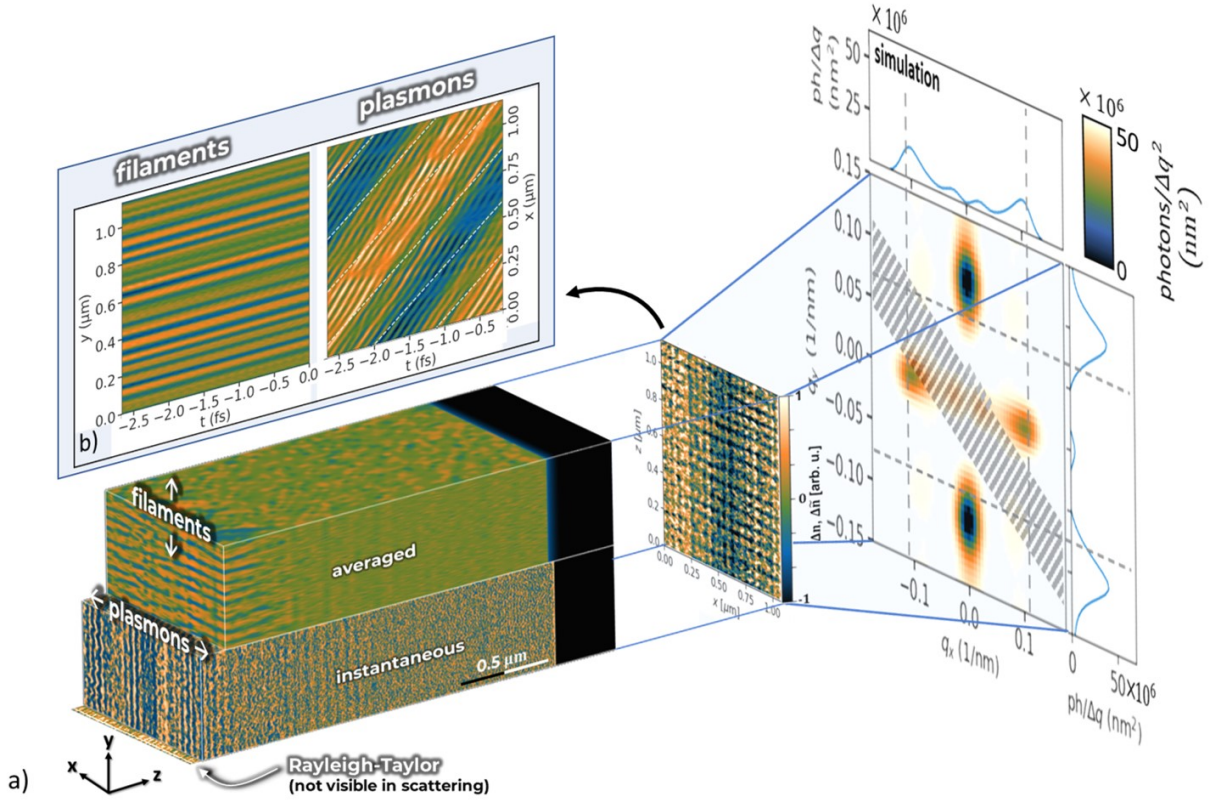


Figure 4. Simulation: **a) Left:** Instantaneous and averaged (over a plasma wavelength of 40 nm) electron density deviation from the average target density close to  $t = 0$ . The superposition of both creates the mesh-like pattern seen in  $\tilde{n}_e$  (**center**). The mesh generates a cross-like pattern in the synthetic scattering signal  $\propto \mathfrak{F}(\tilde{n}_e)$  (**right**). **b)** Time evolution of  $\tilde{n}_e$  averaged along  $x$  (left) and  $y$  (right) show that the filamentation pattern is static while the plasmon features are moving with close to  $\sqrt{2}c$ .

integrated density is measured which would almost completely smear out for the travelling plasmons for probes longer than the plasmon period.

A synthetic scattering pattern comprising 2 laser periods around the peak intensity arrival on target is shown in Fig. 2 and allows a direct comparison with the experiment. The general structures are in exceptional agreement with the experiment, both quantitative and qualitatively. In the horizontal direction the scattering peaks are at the same position in simulation and experiment, while there is a slight mismatch in the vertical direction. Indirect measurements always had the problem that such small deviations could in principle be attributed to the complex processes involved in the measurement, in contrast here we have a clear indication for a different filamentation instability wavelength measured than observed in the simulation. While the scattering angle of the plasmon feature is dictated simply by the experimental geometry, the

position of the filamentation feature is a benchmark for the simulation since it depends on the laser plasma interaction properties via the properties of the laser generated electron current and return current.

Another important aspect is the intensity ratio between the vertical and horizontal signal. While the filamentation instability grows over the full laser pulse duration and beyond, as long as there is a distinct fast forward and bulk return current, the plasmonic signal essentially stops when the laser pulse is over. Hence, at later times we expect the vertical signal to be much larger than the horizontal one, by up to two orders of magnitude at 30 fs after the laser peak based on our simulation. The fact that we do not observe such a strong difference between the vertical and horizontal signal strengths at  $t \approx 0$  is therefore an additional confirmation for having probed the plasma around the laser peak. We expect that with the SAXS technique it will be possible simply by accumulating more shots

– and thereby reducing the timing uncertainty of the average – to directly measure the structure growth rate and hence benchmark the simulated plasma evolution.

In conclusion, combining the experiments, simulations and analytic estimates, we can draw a complete picture of the dominant plasma dynamics in the current experiment: a vertical TSFI with a complex configuration of relativistic forward and return currents and a return bulk current is growing rapidly during the laser irradiation, and horizontal surface plasmons are driven. Both add up to generate a mesh-like electron density pattern that is responsible for the measured cross-like scattering pattern. This is the first ultra-fast dynamic signal visualized by SAXS from UHI laser-driven solids, highlighting the great potential of this novel method. We measured the spatial electron density correlations to few-nanometer, few-femtosecond precision. More comprehensive measurements of the growth rates and spatial scales will allow to refine and benchmark our simulations and overall knowledge of important key topics in relativistic plasma physics, including laser absorption, return current generation, instability growth, and the surface plasmon dispersion relation.

## METHODS

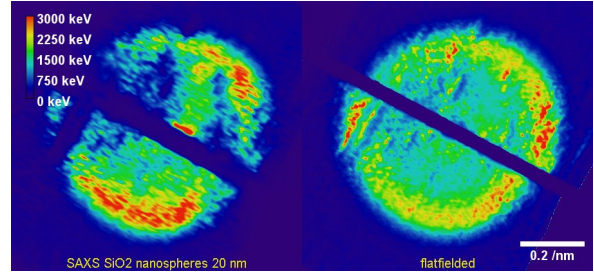
**ReLaX properties:**  $w_L = 4.7 \mu\text{m}$  (focus, FWHM),  $W_L \approx 2.8 \text{ J}$  (pulse energy),  $\tau_L = 30 \text{ fs}$  (pulse duration),  $\lambda_L = 0.8 \mu\text{m}$  (wavelength), calculated intensity  $5 \cdot 10^{20} \text{ W/cm}^2$  ( $a_0 = 15$ ).

**XFEL properties:** SASE beam,  $w_X \approx 20 \mu\text{m}$  (spot size on target, FWHM),  $\tau_X = 30 \text{ fs}$  (pulse duration),  $N_X \approx 7 \cdot 10^{11}$  photons per bunch ( $W_X = 1.5 \text{ mJ}$ ),  $\lambda_X = 0.15 \text{ nm}$  (wavelength) (= 8 keV). The XFEL fundamental was dumped on an X-ray detector 4 m downstream of the target.

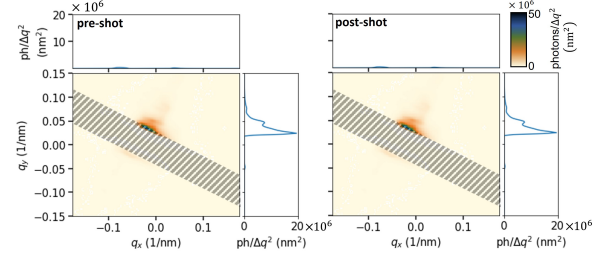
**Synchronization:** The XFEL probe time delay given in the figures is the relative timing measured with the HED optical encoding pulse arrival monitor (PAM) to a precision of 12.9 fs w.r.t. the nominal zero delay set for all runs[34]. The nominal zero delay was not calibrated for the shots in this work, so that this is largely unknown due to drift and the jitter. We therefore give all times relative to the central time between the two highest yield shots.

**SAXS signal processing:** THE SAXS signal is reflected by the HAPG mirror to the Jungfrau detector. The reflectivity of the mirror is approx. 0.2. As the

reflectivity of the mirror is varying over its surface, it has to be corrected by a flat-field inferred from the scattering on a known substance, we employed SiO<sub>2</sub> nanospheres target with particle diameter 20nm, as described in[37]. The geometrical distortion of the signal was also corrected by a scheme described there:



On this corrected data, the signal from XFEL-only pre-shot was subtracted (normalized to the main shot by gas detector measurements for the XFEL intensity), as this resembles the parasitical scattering not originating in the target (see figure below). The background on the data consists mostly of bremsstrahlung generated in the laser-matter interaction and scattered in the chamber, this was subtracted with an uncertainty of approx. 1.3 photons/px. To improve visual readability of Fig. 2, a Gaussian filter of width  $0.002/\text{nm}$  was applied.



**Quantitative analysis of scattering signal:** In Fig. 3 the vertical/horizontal signals were projected along the perpendicular direction over a band 25 px wide around the peaks. Along the vertical/horizontal direction the signal was then integrated around peaks in the region where this projected signal was  $2\sigma$  above the background. The errorbars in the figure indicate the background subtraction uncertainty and Poisson counting statistics. The uncertainty due to the XFEL spatial jitter is not included.

**Simulations:** 3D Simulations were performed using PICongPU[41], spatial resolution  $\Delta x = \Delta y = \Delta z \approx 17 \cdot 2\pi c \omega_{pe}^{-1}$  with  $\omega_{pe} = 20\omega_L$ , and 8 macro ions per cell. The silicon foil was preionized to the +3 state with one macro electron per macro ion (These electrons have an initial temperature  $T_e = 0.1 \text{ keV}$ ). Ionization was included via barrier suppression, ADK and a modified Thomas-Fermi models to correct for low temper-

atures, low densities as described in the PIConGPU documentation. A 50nm exponential preplasma was added to the front target surface to account for ASE and the laser pedestal finite contrast. Additionally, we performed a set of 2D simulations that confirmed that the qualitative results do not sensitively depend on the preplasma in the few 10s of nm scale range. The same is true for hole boring by the spatial intensity profile of the UHI laser: Previous simulations have shown no qualitative change of the dynamics in the small volume around the laser axis between simulations with and without taking into account the pulse shape[36]. The simulated laser is a 30 fs Gaussian p-polarized plane wave with  $a_0 = 15$  peak normalized amplitude propagating at a  $45^\circ$  to the target normal and is initialized  $2.5 \cdot \text{FWHM}$  before and after the max intensity. The transversal box size  $L_{\text{sim},x} = L_{\text{sim},z} = \sqrt{2} \lambda_L$  was chosen to match the laser phase at the periodic boundaries (in the transversal direction),  $L_{\text{sim},y} = 5.08 \lambda_L$ . The field propagation is done with the standard Yee field solver and the absorption at the boundaries in the longitudinal direction is realized with a perfectly matched layer (PML). For particles, we use a 4th order shape together with the Higuera-Cary pusher.

**Synthetic SAXS pattern:** The synthetic SAXS pattern  $I^{\text{synth}}$  was computed by first computing  $\tilde{n}_e$ , and taking its Fourier transform absolute square. The resulting signal was averaged over a time of 3.3 fs. Note that the real XFEL pulse duration was longer, the time here was reduced due to large storage requirement of the 3D data set. To get a quantitative estimate of the expected photons on the detector,  $I^{\text{synth}}$ , the simulated X-ray signal was then scaled to the experimental intensity assuming scattering only within the ReLaX focus (FWHM) with an average half intensity of that in the simulated peak intensity,  $I^{\text{synth}} = N_X (0.5 I_{\text{sim}} / \sum I_{\text{sim}} \cdot w_L)^2 / w_X^2$ . Note: The similarity of the projected plasma wavelength,  $\lambda_x^{\text{PIC}} \cong 2\pi c / \omega_{pe} / \sin \pi/4 = 60 \text{ nm}$ , with the vertical filamentation wavelength  $\lambda_y^{\text{PIC}} = 70 \text{ nm}$  most likely is coincidence, as we repeated the simulation with a more shallow laser incidence angle of  $22.5^\circ$ . There,  $\lambda_x$  is reduced as expected, while  $\lambda_y$  remains constant.

**Identification of the TSFI in the simulation:** We identified three relevant currents: the laser generated fast forward current, the laser generated fast forward current after being reflected at the rear surface, and the bulk return current. The net current is approximately zero. The filaments seen in Fig.4 are quasi-static, growing over time. In the horizontal direction they are not filamented, most likely due to the laser polarization and

finite angle of incidence emitting the electron jets in a number of directions in this plane. The situation in vertical direction is the same as described by Bret[11] except for the fast return current.

**TSFI growth rate:** The growth rate for the TSFI in Eqn. (63) of [11] is given by

$$\Gamma_{\text{TSFI}} \approx \frac{\sqrt{3}}{2^{4/3}} \omega_{pe} \frac{\sqrt[3]{n_b/n_r}}{\gamma_b} = 4.4/\text{fs}. \quad (2)$$

Here,  $\gamma_b \approx \pi / (2K(a_0^2)) = 4.9$  is the average Lorentz factor of the fast electrons[40],  $\omega_{pe}$  is the electron plasma frequency, and  $n_b \approx \gamma_b n_c$ ,  $n_r \approx n_{pe}$ ,  $n_c = 1.7 \cdot 10^{21} / \text{cm}^3$  are the forward, return, and critical density, respectively.

**Why do the plasmons not smear out the signal in SAXS?** While in shadowgraphic methods the XFEL-propagation at a stark angle w.r.t. orientation of the plasmon propagation leads to their contrast almost vanishing for probes longer than the projected plasmon period, for X-ray *scattering*, the signal of a pattern  $\tilde{n}(\mathbf{r})$  moving with velocity  $v_p$  in x-direction is approximately given by the integral over the XFEL irradiated area and XFEL pulse duration

$$I(\mathbf{q}) \propto \int_t \left| \int_w \tilde{n}(\mathbf{r}) e^{i(q_x v_p)t} e^{-i\mathbf{q}\mathbf{r}} d\mathbf{r} \right|^2 dt \propto |FT(\tilde{n}(\mathbf{r}))|^2,$$

i.e. simply the usual Fourier transform absolute square of the static density pattern.

## DATA AVAILABILITY

Data recorded for the experiment at the European XFEL are available at doi:10.22003/XFEL.EU-DATA-002854-00. The processed data and simulation data, as well as the scripts used to generate Figs. 2-4 are available at doi:1014278/rodare/2183.

## ACKNOWLEDGMENTS

We acknowledge European XFEL in Schenefeld, Germany, for provision of X-ray free-electron laser beamtime at HED (High Energy Density Science) HI-BEF (Helmholtz International Beamline for Extreme Fields) SASE2 and would like to thank the staff for their assistance. The authors are indebted to the HI-BEF user consortium for the provision of instrumentation and staff that enabled this experiment. Chris-

tian Gutt acknowledges funding by DFG (GU 535/6-1). This work has also been supported by HIBEF ([www.hibef.eu](http://www.hibef.eu)) and partially by the European Commission via H2020 Laserlab Europe V (PRISES) con-

tract no. 871124, and by the German Federal Ministry of Education and Research (BMBF) under contract number 03Z1O511.

- 
- [1] Florian Kroll, Florian-Emanuel Brack, Constantin Bernert, Stefan Bock, Elisabeth Bodenstein, Kerstin Brüchner, Thomas E. Cowan, Lennart Gaus, René Gebhardt, Uwe Helbig, Leonhard Karsch, Thomas Kluge, Stephan Kraft, Mechthild Krause, Elisabeth Lessmann, Umar Masood, Sebastian Meister, Josefine Metzkes-Ng, Alexej Nossula, Jörg Pawelke, Jens Pietzsch, Thomas Püschel, Marvin Reimold, Martin Rehwald, Christian Richter, Hans-Peter Schlenvoigt, Ulrich Schramm, Marvin E. P. Umlandt, Tim Ziegler, Karl Zeil, and Elke Beyreuther, “Tumour irradiation in mice with a laser-accelerated proton beam,” *Nature Physics* **18**, 316–322 (2022).
- [2] Félicie Albert, M E Couprie, Alexander Debus, Mike C Downer, Jérôme Faure, Alessandro Flacco, Leonida A Gizzi, Thomas Grismayer, Axel Huebl, Chan Joshi, M Labat, Wim P Leemans, Andreas R Maier, Stuart P D Mangles, Paul Mason, François Mathieu, Patric Mugli, Mamiko Nishiuchi, Jens Osterhoff, P P Rajeev, Ulrich Schramm, Jörg Schreiber, Alec G R Thomas, Jean-Luc Vay, Marija Vranic, and Karl Zeil, “2020 roadmap on plasma accelerators,” *New Journal of Physics* **23**, 031101 (2021).
- [3] R. S. Craxton, K. S. Anderson, T. R. Boehly, V. N. Goncharov, D. R. Harding, J. P. Knauer, R. L. McCrory, P. W. McKenty, D. D. Meyerhofer, J. F. Myatt, A. J. Schmitt, J. D. Sethian, R. W. Short, S. Skupsky, W. Theobald, W. L. Kruer, K. Tanaka, R. Betti, T. J. B. Collins, J. A. Delettrez, S. X. Hu, J. A. Marozas, A. V. Maximov, D. T. Michel, P. B. Radha, S. P. Regan, T. C. Sangster, W. Seka, A. A. Solodov, J. M. Soures, C. Stoeckl, and J. D. Zuegel, “Direct-drive inertial confinement fusion: A review,” *Physics of Plasmas* **22**, 110501 (2015).
- [4] C.B. Edwards and C.N. Danson, “Inertial confinement fusion and prospects for power production,” *High Power Laser Science and Engineering* **3**, e4 (2015).
- [5] Alex Zylstra, Neil Alexander, Radha Bahukutumbi, Ryan McBride, Wayne Meier, Peter Seidl, Matt Wolford, and Lin Yin, “IFE Science & Technology Community Strategic Planning Workshop Report (<https://lasers.llnl.gov/content/assets/docs/nif-workshops/ife-workshop-2022/IFE-Workshop-Report.pdf>),” (2022); S C Wilks, A J Kemp, R K Kirkwood, W L Kruer, J D Ludwig, D Mariscal, M Marinak, J Bude, P Patel, P Poole, B Reagan, D Rusby, M Tabak, M Sherlock, R Simpson, T Spinka, V Tang, J Williams, A Friedman, A Zylstra, T Ma, and E Grace, “Short Pulse Laser based Ion Fast Ignition for IFE (<https://lasers.llnl.gov/content/assets/docs/nif-workshops/ife-workshop-2021/white-papers/wilks-LLNL-IFE-workshop-2022.pdf>),” Whitepaper for LLNL-IFE-workshop (2022); L. Obst-Huebl, S Hakimi, K Nakamura, T Ostermayr, J Van Tilborg, S Bulanov, A Huebl, V Tang, J Williams, A Friedman, T Ma, and E Grace, “BELLA PW 1 Hz Laser Experiments for Short Pulse Laser-based Ion Fast Ignition for IFE (<https://lasers.llnl.gov/content/assets/docs/nif-workshops/ife-workshop-2021/white-papers/obsthuebl-LBNL-IFE-workshop-2022.pdf>),” , 1–10 (2022).
- [6] H. Abu-Shawareb, R. Acree, P. Adams, J. Adams, B. Addis, and A. B. Zylstra, “Lawson Criterion for Ignition Exceeded in an Inertial Fusion Experiment,” *Physical Review Letters* **129**, 075001 (2022).
- [7] Breanna Bishop (LLNL press release: <https://www.llnl.gov/news/national-ignition-facility-achieves-fusion-ignition>), “National Ignition Facility achieves fusion ignition,” (2022).
- [8] S. H. Glenzer, B. J. MacGowan, P. Michel, N. B. Meezan, L. J. Suter, S. N. Dixit, J. L. Kline, G. A. Kyrala, D. K. Bradley, D. A. Callahan, E. L. Dewald, L. Divol, E. Dzenitis, M. J. Edwards, A. V. Hamza, C. A. Haynam, D. E. Hinkel, D. H. Kalantar, J. D.ilkenny, O. L. Landen, J. D. Lindl, S. LePape, J. D. Moody, A. Nikroo, T. Parham, M. B. Schneider, R. P. J. Town, P. Wegner, K. Widmann, P. Whitman, B. K. F. Young, B. Van Wonterghem, L. J. Atherton, and E. I. Moses, “Symmetric Inertial Confinement Fusion Implosions at Ultra-High Laser Energies,” *Science* **327**, 1228–1231 (2010).
- [9] M. Roth, T. E. Cowan, M. H. Key, S. P. Hatchett, C. Brown, W. Fountain, J. Johnson, D. M. Pennington, R. A. Snavely, S. C. Wilks, K. Yasuike, H. Ruhl, F. Pegoraro, S. V. Bulanov, E. M. Campbell, M. D. Perry, and H. Powell, “Fast ignition by intense laser-accelerated proton beams,” *Physical Review Letters* **86**, 436–439 (2001).
- [10] E. M. Campbell, T. C. Sangster, V. N. Goncharov, J. D. Zuegel, S. F.B. Morse, C. Sorce, G. W. Collins, M. S. Wei, R. Betti, S. P. Regan, D. H. Froula, C. Dorrer, D. R. Harding, V. Gopalaswamy, J. P. Knauer, R. Shah, O. M. Mannion, J. A. Marozas, P. B. Radha, M. J. Rosenber, T. J.B. Collins, A. R. Christopherson, A. A. Solodov, D. Cao, J. P. Palastro, R. K. Follett, and M. Farrell, “Direct-drive laser fusion: status, plans and future,”



- Philosophical Transactions of the Royal Society A **379** (2021), 10.1098/RSTA.2020.0011.
- [11] A. Bret, M. C. Firpo, and C. Deutsch, "Collective electromagnetic modes for beam-plasma interaction in the whole [Formula presented] space," *Physical Review E - Statistical Physics, Plasmas, Fluids, and Related Interdisciplinary Topics* **70**, 15 (2004).
- [12] J. Metzkes, T. Kluge, K. Zeil, M. Bussmann, S. D. Kraft, T. E. Cowan, and U. Schramm, "Experimental observation of transverse modulations in laser-driven proton beams," *New Journal of Physics* **16**, 23008 (2014).
- [13] S. Göde, C. Rödel, K. Zeil, R. Mishra, M. Gauthier, F.-E. Brack, T. Kluge, M.J. J. MacDonald, J. Metzkes, L. Obst, M. Rehwald, C. Ruyer, H.-P. P. Schlenvoigt, W. Schumaker, P. Sommer, T.E. E. Cowan, U. Schramm, S. Glenzer, and F. Fiuza, "Relativistic electron streaming instabilities modulate proton beams accelerated in laser-plasma interactions," *Physical Review Letters* **118**, 194801 (2017).
- [14] G. G. Scott, C. M. Brenner, V. Bagnoud, R. J. Clarke, B. Gonzalez-Izquierdo, J. S. Green, R. I. Heathcote, H. W. Powell, D. R. Rusby, B. Zielbauer, P. McKenna, and D. Neely, "Diagnosis of Weibel instability evolution in the rear surface density scale lengths of laser solid interactions via proton acceleration," *New Journal of Physics* **19**, 043010 (2017).
- [15] L. G. Huang, H. P. Schlenvoigt, H. Takabe, and T. E. Cowan, "Ionization and reflux dependence of magnetic instability generation and probing inside laser-irradiated solid thin foils," *Physics of Plasmas* **24**, 103115 (2017).
- [16] Andrea Macchi, Fulvio Cornolti, and Francesco Pegoraro, "Two-surface wave decay," *Physics of Plasmas* **9**, 1704–1711 (2002).
- [17] C. A.J. Palmer, J. Schreiber, S. R. Nagel, N. P. Dover, C. Bellei, F. N. Beg, S. Bott, R. J. Clarke, A. E. Dangor, S. M. Hassan, P. Hilz, D. Jung, S. Kneip, S. P.D. Mangles, K. L. Lancaster, A. Rehman, A. P.L. Robinson, C. Spindloe, J. Szerypo, M. Tatarakis, M. Yeung, M. Zepf, and Z. Najmudin, "Rayleigh-Taylor instability of an ultrathin foil accelerated by the radiation pressure of an intense laser," *Physical Review Letters* **108**, 225002 (2012).
- [18] T. Kluge, J. Metzkes, K. Zeil, M. Bussmann, U. Schramm, and T. E. Cowan, "Two surface plasmon decay of plasma oscillations," *Physics of Plasmas* **22**, 64502 (2015).
- [19] A. Sgattoni, S. Sinigardi, L. Fedeli, F. Pegoraro, and A. Macchi, "Laser-driven Rayleigh-Taylor instability: Plasmonic effects and three-dimensional structures," *Physical Review E - Statistical, Nonlinear, and Soft Matter Physics* **91**, 013106 (2015).
- [20] K. Sokolowski-Tinten, J. Bialkowski, A. Cavalleri, D. Von der Linde, A. Oparin, J. Meyer-Ter-Vehn, and S. I. Anisimov, "Transient States of Matter during Short Pulse Laser Ablation," *Physical Review Letters* **81**, 224 (1998).
- [21] J. P. Geindre, A. Mysyrowicz, A. Dos Santos, P. Audebert, A. Rousse, G. Hamoniaux, A. Antonetti, F. Falliès, and J. C. Gauthier, "Frequency-domain interferometer for measuring the phase and amplitude of a femtosecond pulse probing a laser-produced plasma," *Optics Letters* **19**, 1997 (1994); Maïmouna Bocoum, Frederik Böhle, Aline Vernier, Aurélie Jullien, Jérôme Faure, and Rodrigo Lopez-Martens, "Spatial-domain interferometer for measuring plasma mirror expansion," *Optics Letters* **40**, 3009 (2015).
- [22] A. Malvache, A. Borot, F. Quéré, and R. Lopez-Martens, "Coherent wake emission spectroscopy as a probe of steep plasma density profiles," *Physical Review E - Statistical, Nonlinear, and Soft Matter Physics* **87**, 035101 (2013).
- [23] K. Quinn, L. Romagnani, B. Ramakrishna, G. Sarri, M. E. Dieckmann, P. A. Wilson, J. Fuchs, L. Lancia, A. Pipahl, T. Toncian, O. Willi, R. J. Clarke, M. Notley, A. MacChi, and M. Borghesi, "Weibel-induced filamentation during an ultrafast laser-driven plasma expansion," *Physical Review Letters* **108**, 135001 (2012).
- [24] L. B. Fletcher, H. J. Lee, T. Döppner, E. Galtier, B. Nagler, P. Heimann, C. Fortmann, S. LePape, T. Ma, M. Millot, A. Pak, D. Turnbull, D. A. Chapman, D. O. Gericke, J. Vorberger, T. White, G. Gregori, M. Wei, B. Barbrel, R. W. Falcone, C. C. Kao, H. Nuhn, J. Welch, U. Zastra, P. Neumayer, J. B. Hastings, and S. H. Glenzer, "Ultrabright X-ray laser scattering for dynamic warm dense matter physics," *Nature Photonics* **9**, 274–279 (2015).
- [25] Tais Gorkhover, Sebastian Schorb, Ryan Coffee, Marcus Adolph, Lutz Foucar, Daniela Rupp, Andrew Aquila, John D. Bozek, Sascha W. Epp, Benjamin Erk, Lars Gumprecht, Lotte Holmegaard, Andreas Hartmann, Robert Hartmann, Günter Hauser, Peter Holl, Andre Hömke, Per Johnsson, Nils Kimmel, Kai Uwe Kühnel, Marc Messerschmidt, Christian Reich, Arnaud Rouzée, Benedikt Rudek, Carlo Schmidt, Joachim Schulz, Heike Soltau, Stephan Stern, Georg Weidenspointner, Bill White, Jochen Küpper, Lothar Strüder, Ilme Schlichting, Joachim Ullrich, Daniel Rolles, Artem Rudenko, Thomas Möller, and Christoph Bostedt, "Femtosecond and nanometre visualization of structural dynamics in superheated nanoparticles," *Nature Photonics* **10**, 93–97 (2016).
- [26] T. Kluge, C. Rödel, M. Rödel, A. Pelka, E. E. McBride, L. B. Fletcher, M. Harmand, A. Krygier, A. Higginbotham, M. Bussmann, E. Galtier, E. Gamboa, A. L. Garcia, M. Garten, S. H. Glenzer, E. Granos, C. Gutt, H. J. Lee, B. Nagler, W. Schumaker, F. Tavella, M. Zacharias, U. Schramm, and T. E. Cowan, "Nanometer-scale characterization of laser-driven compression, shocks, and phase transitions, by x-ray scattering using free electron lasers," *Physics of Plasmas* **24**, 102709 (2017).

- [27] Thomas Kluge, Melanie Rödel, Josefine Metzkes-Ng, Alexander Pelka, Alejandro Laso Garcia, Irene Prencipe, Martin Rehwald, Motoaki Nakatsutsumi, Emma E. McBride, Tommy Schönherr, Marco Garten, Nicholas J. Hartley, Malte Zacharias, Jörg Grenzer, Artur Erbe, Yordan M. Georgiev, Eric Galtier, Inhyuk Nam, Hae Ja Lee, Siegfried Glenzer, Michael Bussmann, Christian Gutt, Karl Zeil, Christian Rödel, Uwe Hübner, Ulrich Schramm, and Thomas E. Cowan, “Observation of Ultrafast Solid-Density Plasma Dynamics Using Femtosecond X-Ray Pulses from a Free-Electron Laser,” *Physical Review X* **8**, 031068 (2018).
- [28] Mianzhen Mo, Samuel Murphy, Zhijiang Chen, Paul Fossati, Renkai Li, Yongqiang Wang, Xijie Wang, and Siegfried Glenzer, “Visualization of ultrafast melting initiated from radiation-driven defects in solids,” *Science Advances* **5** (2019), 10.1126/sciadv.aaw0392.
- [29] Lennart Gaus, Lothar Bischoff, Michael Bussmann, Eric Cunningham, Chandra B. Curry, Juncheng E, Eric Galtier, Maxence Gauthier, Alejandro Laso García, Marco Garten, Siegfried Glenzer, Jörg Grenzer, Christian Gutt, Nicholas J. Hartley, Lingen Huang, Uwe Hübner, Dominik Kraus, Hae Ja Lee, Emma E. McBride, Josefine Metzkes-Ng, Bob Nagler, Motoaki Nakatsutsumi, Jan Nikl, Masato Ota, Alexander Pelka, Irene Prencipe, Lisa Randolph, Melanie Rödel, Youichi Sakawa, Hans-Peter Peter Schlenvoigt, Michal Šmíd, Franziska Treffert, Katja Voigt, Karl Zeil, Thomas E. Cowan, Ulrich Schramm, Thomas Kluge, J. E. Juncheng, Eric Galtier, Maxence Gauthier, Alejandro Laso García, Marco Garten, Siegfried Glenzer, Jörg Grenzer, Christian Gutt, Nicholas J. Hartley, Lingen Huang, Uwe Hübner, Dominik Kraus, Hae Ja Lee, Emma E. McBride, Josefine Metzkes-Ng, Bob Nagler, Motoaki Nakatsutsumi, Jan Nikl, Masato Ota, Alexander Pelka, Irene Prencipe, Lisa Randolph, Melanie Rödel, Youichi Sakawa, Hans-Peter Peter Schlenvoigt, Michal Šmíd, Franziska Treffert, Katja Voigt, Karl Zeil, Thomas E. Cowan, Ulrich Schramm, and Thomas Kluge, “Probing ultrafast laser plasma processes inside solids with resonant small-angle x-ray scattering,” *Physical Review Research* **3**, 043194 (2021).
- [30] A. Laso Garcia, H. Höppner, A. Pelka, C. Bähtz, E. Brambrink, S. Di Dio Cafiso, J. Dreyer, S. Göde, M. Hassan, T. Kluge, J. Liu, M. Makita, D. Möller, M. Nakatsutsumi, T. R. Preston, G. Priebe, H. P. Schlenvoigt, J. P. Schwinkendorf, M. Šmíd, A. M. Talposi, M. Toncian, U. Zastrau, U. Schramm, T. E. Cowan, and T. Toncian, “ReLaX: the Helmholtz International Beamline for Extreme Fields high-intensity short-pulse laser driver for relativistic laser–matter interaction and strong-field science using the high energy density instrument at the European X-ray free electron laser fa,” *High Power Laser Science and Engineering* **9**, E59 (2021).
- [31] HIBEF Consortium, “<http://www.hibef.eu>,”.
- [32] M. Nakatsutsumi and Th. Tschentscher, *Conceptual design report: scientific instrument high energy density physics (HED)*, Tech. Rep. (European X-Ray Free-Electron Laser Facility GmbH, 2013).
- [33] Ulf Zastrau, Karen Appel, Carsten Baecht, Oliver Baehr, Lewis Batchelor, Andreas Berghäuser, Mohammadreza Banjafar, Erik Brambrink, Valerio Cerantola, Thomas E. Cowan, Horst Damker, Steffen Dietrich, Samuele Di Dio Cafiso, Jörn Dreyer, Hans Olaf Engel, Thomas Feldmann, Stefan Findeisen, Manon Foesé, Daniel Fulla-Marsa, Sebastian Göde, Mohammed Hassan, Jens Hauser, Thomas Herrmannsdörfer, Hauke Höppner, Johannes Kaa, Peter Kaefer, Klaus Knöfel, Zuzana Konopková, Alejandro Laso García, Hanns Peter Liermann, Jona Mainberger, Mikako Makit, Eike Christian Martens, Emma E. McBride, Dominik Möller, Motoaki Nakatsutsumi, Alexander Pelka, Christian Plueckthun, Clemens Prescher, Thomas R. Preston, Michael Röper, Andreas Schmidt, Wolfgang Seidel, Jan Patrick Schwinkendorf, Markus O. Schoelmerich, Ulrich Schramm, Andreas Schropp, Cornelius Strohm, Konstantin Sukharnikov, Peter Talkovski, Ian Thorpe, Monika Toncian, Toma Toncian, Lennart Wollenweber, Shingo Yamamoto, and Thomas Tschentscher, “The High Energy Density Scientific Instrument at the European XFEL,” *urn:issn:1600-5775* **28**, 1393–1416 (2021).
- [34] A. Laso Garcia, H. Höppner, A. Pelka, C. Bähtz, E. Brambrink, S. Di Dio Cafiso, J. Dreyer, S. Göde, M. Hassan, T. Kluge, J. Liu, M. Makita, D. Möller, M. Nakatsutsumi, T. R. Preston, G. Priebe, H.-P. Schlenvoigt, J.-P. Schwinkendorf, M. Šmíd, A.-M. Talposi, M. Toncian, U. Zastrau, U. Schramm, T. E. Cowan, and T. Toncian, “ReLaX: the Helmholtz International Beamline for Extreme Fields high-intensity short-pulse laser driver for relativistic laser–matter interaction and strong-field science using the high energy density instrument at the European X-ray free electron laser fa,” *High Power Laser Science and Engineering* **9**, e59 (2021).
- [35] A. Bret, L. Gremillet, and D. Bénisti, “Exact relativistic kinetic theory of the full unstable spectrum of an electron-beam–plasma system with Maxwell-Jüttner distribution functions,” *Physical Review E* **81**, 036402 (2010).
- [36] T. Kluge, C. Gutt, L. G. Huang, J. Metzkes, U. Schramm, M. Bussmann, and T. E. Cowan, “Using X-ray free-electron lasers for probing of complex interaction dynamics of ultra-intense lasers with solid matter,” *Physics of Plasmas* **21**, 033110 (2014).
- [37] M. Šmíd, C. Baecht, A. Pelka, A. Laso García, S. Göde, J. Grenzer, T. Kluge, Z. Konopkova, M. Makita, I. Prencipe, T. R. Preston, M. Rödel, and T. E. Cowan, “Mirror to measure small angle x-ray scattering signal in high energy density experiments,” *Review of Scientific Instruments* **91**, 123501 (2020).

- [38] F. Califano, R. Prandi, F. Pegoraro, and S. V. Bulanov, "Nonlinear filamentation instability driven by an inhomogeneous current in a collisionless plasma," *Physical Review E* **58**, 7837–7845 (1998).
- [39] Mikhail V. Medvedev and Abraham Loeb, "Generation of Magnetic Fields in the Relativistic Shock of Gamma-Ray Burst Sources," *The Astrophysical Journal* **526**, 697–706 (1999).
- [40] T. Kluge, T. Cowan, A. Debus, U. Schramm, K. Zeil, and M. Bussmann, "Electron Temperature Scaling in Laser Interaction with Solids," *Physical Review Letters* **107**, 205003 (2011).
- [41] "PICongGPU – A Many-GPGPU Particle-in-Cell Code: <http://picongpu.hzdr.de>," (2017).